Broadband dielectric measurements on the (*R*)-1-methylheptyl-6-(4′-decyloxybenzoyloxy)-2-naphthalene carboxylate antiferroelectric liquid crystal

S. Merino,[1] M. R. de la Fuente,[1] Y. González,[1] M. A. Pérez Jubindo,[1] B. Ros,[2] and J. A. Puértolas[3]
[1]*Departamento de Física Aplicada II, Facultad de Ciencias, Universidad del País Vasco, Apartado 644, E-48080 Bilbao, Spain*
[2]*Departamento de Química Orgánica, Instituto de Ciencia de Materiales de Aragón, Facultad de Ciencias, Universidad de Zaragoza, Consejo Superior de Investigaciones Científicas, E-50009 Zaragoza, Spain*
[3]*Departamento de Ciencia y Tecnología de Materiales y Fluidos, Centro Politécnico Superior, Universidad de Zaragoza, E-50015 Zaragoza, Spain*
(Received 5 January 1996)

We have studied by means of polarization, tilt and broadband dielectric spectroscopy the liquid crystal (*R*)-1-methylheptyl-6-(4′-decyloxybenzoyloxy)-2-naphthalene carboxylate. This compound together with a ferrielectric and two antiferroelectric phases shows a broad range, 6 °C, of Sm-C^*_α phase. The dielectric study shows the presence of a Goldstone mode in the latter mesophase, which in turn would confirm its tilted and helical nature. Other collective modes, such as the soft mode and a mode related to the antiferroelectric ordering and the helical structure, have also been characterized. With respect to the molecular modes, the rotation around the molecular long axis has been studied from the isotropic to the low temperature antiferroelectric phase. This study shows that the molecules are quite rigid and that the dynamics of the motions around the molecular long axis is not greatly influenced by the transitions among the different smectic mesophases. In particular, the thermal activation energy of the process is the same in the paraelectric Sm-*A* phase and in the complex Sm-C^*_α phase. However, the frequency shows a jump at the Sm-$C^*_\gamma \rightarrow$ Sm-C^*_A phase transition, which could be due to an increase of the order of the molecular short axes. [S1063-651X(96)11510-5]

PACS number(s): 61.30.−v, 77.22.Gm, 77.80.−e

INTRODUCTION

Since the first antiferroelectric liquid-crystalline phase was discovered by Chandani *et al.* in 1989 [1,2], a large amount of new series of materials showing ferroelectric, ferrielectric, and antiferroelectric mesophases have been found. In spite of the large amount of experimental and theoretical work devoted to this subject, a clear explanation of the structure of these new phases has not yet been achieved. The phenomenology they exhibit is complex: many transitions that cannot be detected by means of the usual characterization techniques, such as x-ray or differential scanning calorimetry [3,4], transition temperature changes with the cell thickness, anomalous behavior of the helical pitch [5], phases that disappear changing the optical purity [6], different (qualitative and quantitative) results in the same phase of different compounds [7,8], etc. Dielectric and electro-optic experiments have become very important in this field because of their capability of providing information about the collective modes involved in these polar phases: soft mode, ferroelectric Goldstone mode, helix related ferrielectric and antiferroelectric modes, etc. [4,9–16].

In this paper we will show experimental results on the compound with chemical formula (hereafter called ICOOET)

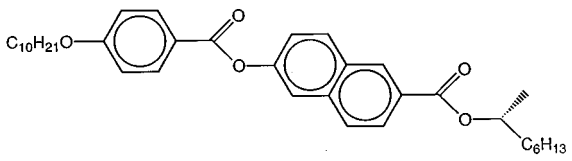

This compound appeared in the literature in 1991 [17] but the reported phase sequence was $I \rightarrow$ Sm-$A \rightarrow$ Sm-$C^* \rightarrow C$ (crystalline). Our (dielectric) results show that it also has ferrielectric and antiferroelectric mesophases:

$$I \xrightarrow[64.5\ ^\circ\mathrm{C}]{} \text{Sm-}A \xrightarrow[48\ ^\circ\mathrm{C}]{} \text{Sm-}C^*_\alpha \xrightarrow[41.8\ ^\circ\mathrm{C}]{} \text{AF} \xrightarrow[32\ ^\circ\mathrm{C}]{} \text{Sm-}C^*_\gamma \xrightarrow[27.7\ ^\circ\mathrm{C}]{} \text{Sm-}C^*_A \xrightarrow[23\ ^\circ\mathrm{C}]{} C.$$

It is worth noticing that it does not show the Sm-C^* phase. Instead it has a Sm-C^*_α phase during a broad range of temperature, near 6°. It also shows a reentrant antiferroelectric AF phase [18].

The structure of the Sm-C^*_A phase was found to be antiferroelectrically ordered with molecules in adjacent layers tilted in opposite directions [1,2]. The Sm-C^*_γ is ferrielectric and models consisting of an alternate sequence of ferro and antiferroelectric ordering were proposed [19]. Thus, the unit cell consists of three (or more) layers such that the tilt in two of them points in one direction and in the third one in the opposite. Recently, other authors [4] have proposed a bilayer structure to account for the Sm-$C^* \rightarrow$ Sm-$C^*_\gamma \rightarrow$ Sm-C^*_A phase sequence, being an azimuthal reorientation of the molecules at the transitions the mechanism that originates the different phases. Still more controversy exists about the Sm-C^*_α phase. Its presence is related to a reduce ability of the material to form ferroelectric Sm-C^* and antiferroelectric Sm-C^*_A [19]. The interaction between smectic layers due to collective polarization fluctuations causes the antiferroelectricity in the high-temperature region of the Sm-C^*_α phase. The competition between this antiferroelectricity and the ferroelectricity causes the complexity of the Sm-C^*_α phase. Cepic and Zeks [20] have analyzed the discrete model

proposed by Sun, Orihara, and Ishibashi [21] that takes into account interlayer interactions between the nearest and the next-nearest neighboring layers. The model predicts for the Sm-C^*_α phase a short pitch tilted phase due to the competition between the interlayer interactions when the next nearest one favor antiparallel orientation. When this interaction becomes larger the structure has four layer period and an antiferroelectric character: adjacent layers tilt in directions making a 90° angle. These authors suggest that this structure could be the high-temperature antiferroelectric phase (AF) in contrast with the model proposed by Fukuda *et al.* [19] and Isozaki *et al.* [22] in which the layers form pairs; the two members of a pair tilt in the same direction and the adjacent pair in the opposite direction. The latter model explains all the possible phases observed in this type of material: Sm-$C^*_\alpha \rightarrow$ Sm-$C^* \rightarrow$ AF$\rightarrow$ FI$_H$ (ferrielectric high temperature) $\rightarrow$ Sm-$C^*_\gamma \rightarrow$ FI$_L$ (ferrielectric low temperature) $\rightarrow$ Sm-C^*_A, as due to a competition between antiferroelectric and ferroelectric interactions stabilizing Sm-C^*_A and Sm-C^* phases, respectively, in the same way as previously was explained the complex Sm-C^*_α phase. A devil staircase, derived from the Sm-C^*_A is introduced being Sm-$C^*_A(0)$ = Sm-C^*_A, Sm-$C^*_A(1)$ = Sm-C^*, Sm-$C^*_A(\frac{1}{3})$ = Sm-C^*_γ, Sm-$C^*_A(\frac{1}{2})$ = AF, and so on. This structure would explain, for example, the observed behavior of the apparent tilt angle versus field in the different phases. In this paper we report polarization, tilt, and dielectric studies in ICOOET.

EXPERIMENT

The ICOOET was obtained following a synthetic pathway similar to the one described for its biphenyl homologous [2,14]. The intermediates and the final compound were all characterized by microanalysis for which satisfactory results were determined. The data obtained by IR, NMR, and mass spectroscopy were found to be consistent with the predicted structures of the products. Purity of the materials was checked by thin-layer chromatography and high-pressure liquid chromatography showing a chemical purity exceeding 99.5%. For the synthesis we used the commercially available (*S*)-(+)-2-octanol (Aldrich), which served as an enantiomerically enriched starting material. The esterification reaction was carried out following the procedure described by Mitsunobu [23]. This is a redox reaction which proceeds with net inversion of configuration in the chiral center. The pure final product was twice recrystallyzed from absolute ethanol. Optical purity of the compound was determined by polarimetry and ^{1}H NMR using shift reagent and comparing with the racemic samples. Based on these results we assumed that the final compound was essentially optically pure.

Three different measuring systems were used to measure the complex dielectric permittivity over nine decades of frequency (10^0–10^9 Hz): a Schlumberger 1260 frequency response analyzer (10^0–10^4 Hz) and two impedance analyzers: HP 4192A (10^2–10^7 Hz) and HP 4192A (10^6–10^9 Hz). The HP 4192A measures the impedance of the sample from the reflection coefficient at the end of a 50 Ω coaxial transmission line. With this setup high conductivity electrodes must be used. In order to guarantee the same alignment conditions over the whole frequency range, the same cell must be used with the three measuring systems. Thus, the cell consists of two gold plated brass electrodes (with a diameter of 5 mm) separated by 50-μm-thick silica spacers. The spontaneous polarization was measured, using the triangular wave method, for different values of the frequency and maximum voltages in order to properly characterize the different reorientation processes. In this case commercially available cells with transparent indium tin oxide (ITO) electrodes, coated with polyimide and having the cell thickness of 25 μm were used. These cells were also used for the dielectric study under biasing fields in order to control its effect on the helical structure. It is worth noticing that the alignment was not perfect, always showing a fan-shaped texture.

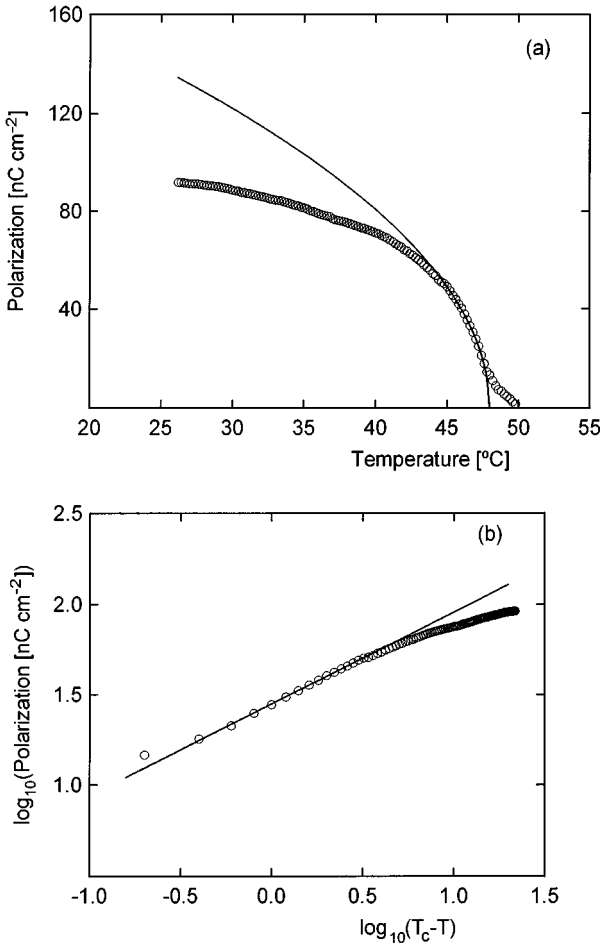

FIG. 1. Spontaneous polarization vs temperature. Measuring conditions: triangular field, maximum field 9 V μm^{-1}, 50 Hz, solid line: fitting to Eq. (1). (a) linear, (b) log$_{10}$-log$_{10}$ plot.

RESULTS

Figure 1(a) shows the spontaneous polarization P_S versus temperature. The frequency of the triangular wave was 50 Hz and the maximum field value 9 V μm^{-1}. This field is high enough to switch the antiferro an ferrielectric states to the ferroelectric ones, and then no anomaly could be detected on the $P_S(T)$ curve at the phase transitions. The continuous line is the fit to the power law

$$P_s(T) = P_0(T_C - T)^\beta, \tag{1}$$

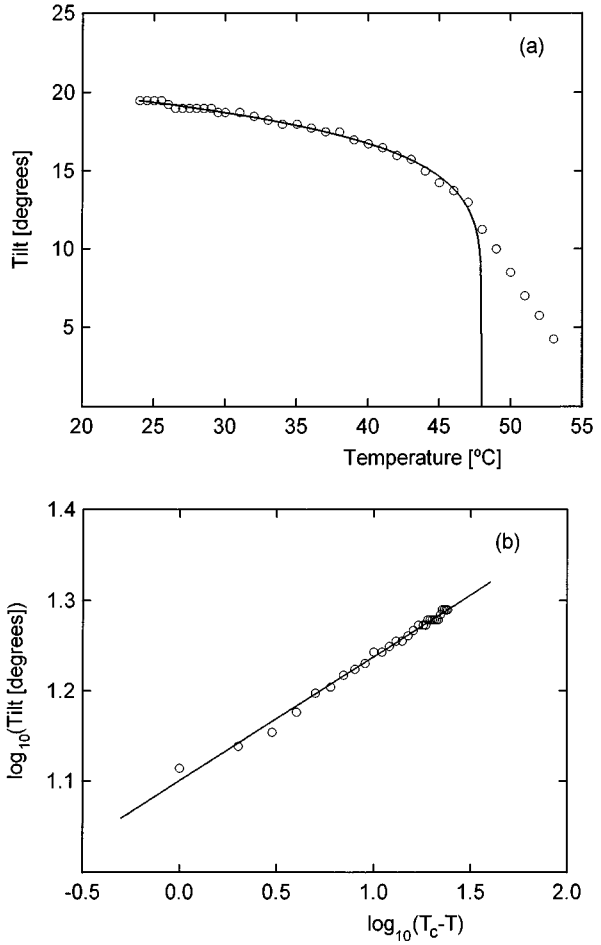

FIG. 2. Apparent tilt angle vs temperature. Measuring conditions: square field ± 6 V μm^{-1}. Solid line: fitting to Eq. (2). (a) linear, (b) $\log_{10}$-$\log_{10}$ plot.

with $P_0=28.05$ nCcm^{-2}, $\beta=0.5$, and $T_c=48$ °C, in a perfect agreement with the mean field model. Figure 1(b) shows the same as Fig. 1(a) but in a $\log_{10}$-$\log_{10}$ plot. The apparent tilt angle of the molecules from the normal to the smectic layers, θ, was measured using a square wave of ∓ 6 V μm^{-1} in order to guarantee the switching to the ferroelectric states and is represented versus temperature in Fig. 2(a). Figure 2(b) shows the corresponding $\log_{10}$-$\log_{10}$ plot. No anomaly could be detected in the $\theta(T)$ curve at the phase transitions. The whole temperature range could be fitted to the power law

$$\theta(T)=\theta_0(T_C-T)^{\beta}, \tag{2}$$

with $T_c=48$ °C, $\theta_0=12.6$ °, and $\beta=0.14$, a value very far from the mean field value obtained for the polarization. It is worth noticing the high value of the apparent tilt in the Sm-A phase, indicating an important electroclinic effect, in part due to the high value of the measuring field. The same effect is included in the Sm-C^*_α phase, which would explain the high value of the apparent tilt near the Sm-A phase and the small value of the β parameter. From the analysis of the current-field cycles for different maximum fields and frequencies we arrived at an identification of the different phases. When in these cycles, upon cooling from the Sm-A phase, the reversal of the spontaneous polarization starts to

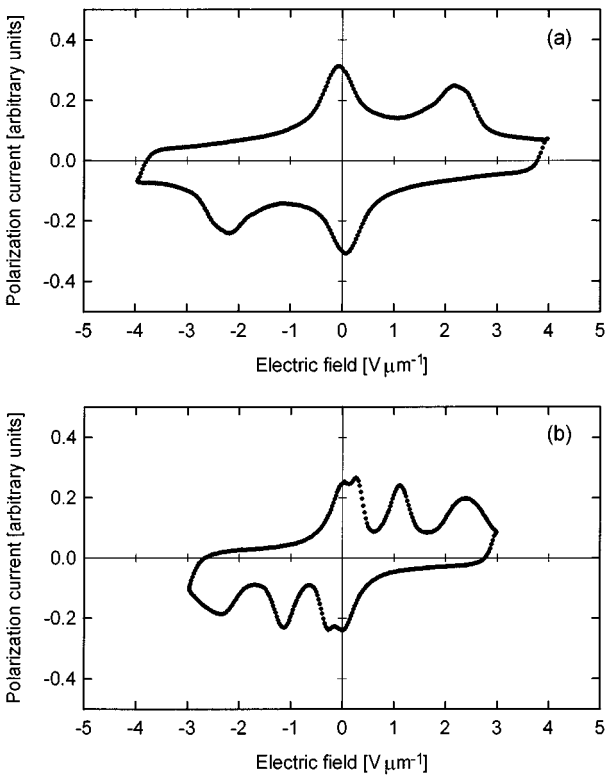

FIG. 3. Current-field cycles. Measurement conditions: triangular field, frequency 50 Hz. (a) on the high-temperature side of the Sm-C^*_α phase, showing its antiferroelectriclike character; (b) in the AF phase, showing four peaks.

appear: two clear peaks, instead of one, are observed [see Fig. 3(a)]. These are present for different frequencies of the applied triangular field. When the temperature goes down one peak decreases and the other increases. This is in accordance with similar measurements in other compounds with Sm-C^*_α phase, where an antiferroelectriclike behavior is observed near the paraelectric phase and a progressive change to ferrielectric behavior occurs as the temperature goes down [19,24]. Around 42 °C the pattern of the reversal of the polarization changes. We observed several peaks depending on the field and frequency. In Fig. 3(b) four peaks were obtained. As Fukuda, Takanishi, and Ishikawa mentioned in [19], more than four states and three peaks may appear in the switching because the field-induced transition may occur in such a way that an antiferroelectric phase (a ferrielectric phase) may transform into the ferroelectric phase indirectly via a ferrielectric phase (another ferrielectric phase). This behavior was assigned to the AF phase.

Figure 4(a) shows the apparent tilt angle (normalized to the saturation value) for different values of the electric field in the Sm-C^*_α (47 °C), AF (35 °C), Sm-C^* (30 °C), and Sm-C^*_A (26 °C) phases. The stepwise increase is evident, indicating that there are several intermediate steps induced by an electric field. In both antiferroelectric mesophases there is a critical field below which the apparent tilt is zero. The value in the plateau corresponds to $\frac{1}{3}$ of the saturation value, the same as in the Sm-C^*_γ phase [24,25]. However, in the high-temperature side of the AF phase the behavior is similar to the Sm-C^*_α phase, in which the plot shows more steps in accordance with its complex nature. The field depen-

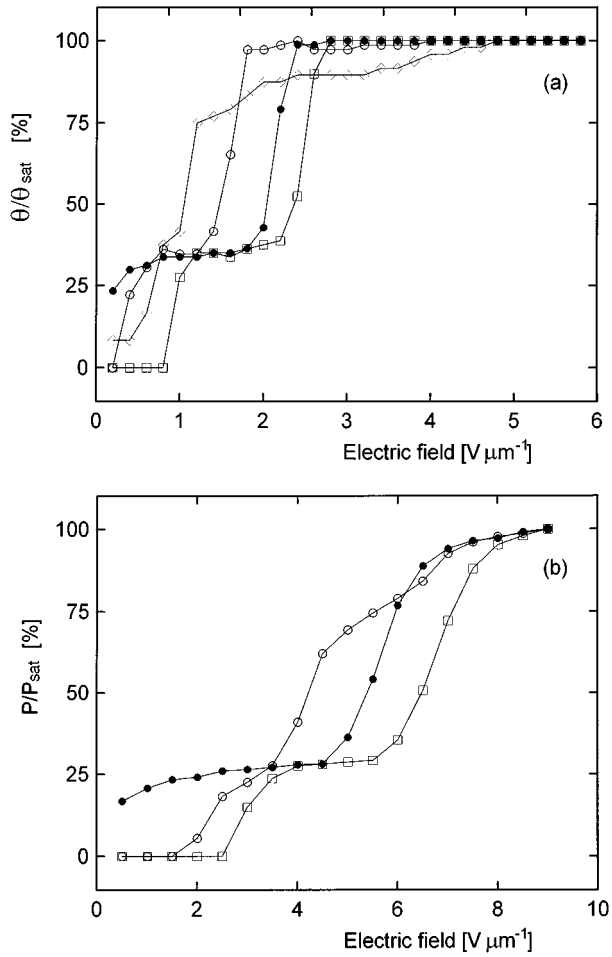

FIG. 4. (a) Measured apparent tilt angle (normalized with the saturation value) vs applied electric field for different temperatures: (◇) 47 °C in the Sm-C^*_α phase; (○) 35 °C in the AF phase; (●) 30 °C in the Sm-C^*_γ phase; (□) 26 °C in the Sm-C^*_A phase. (b) Measured polarization (normalized with the saturation value) vs maximum triangular field: (○) 35 °C in the AF phase; (●) 30 °C in the Sm-C^*_γ phase; (□) 26 °C in the Sm-C^*_A phase.

dence of the measured polarization shows similar effects as the apparent tilt angle [see Fig. 4(b)]. Note that the fields are not comparable because in the case of the polarization it was triangular and the critical fields are also frequency dependent.

Figure 5 shows a tridimensional plot of the dielectric losses, ε'', versus temperature and frequency (10^2–10^9 Hz). The high frequency relaxation is related to the rotation around molecular long axis. The low frequency relaxations are a mixture of different modes (soft mode and helix related modes) that we will discuss later. In this low frequency region the different transitions can be seen. The maximum corresponds to the Sm-$A \rightarrow$Sm-C^*_α phase transition. The following decrease on decreasing temperature is the onset of the AF phase and the increase in the very low frequency region corresponds to the onset of the Sm-C^*_γ phase.

Now we will analyze deeply the dielectric behavior in the different phases. Dielectric data for low-molar-weight liquid crystals are in general well described assuming the small step rotational diffusion model for the molecular dynamics. In this theory each molecule is supposed to act independently of

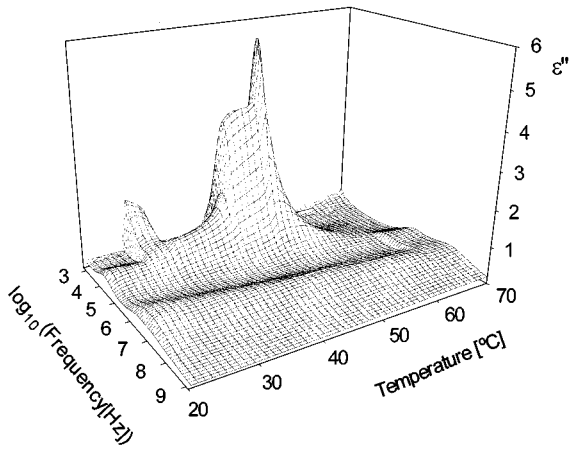

FIG. 5. Dielectric losses vs temperature and frequency.

its neighbors, which just contributes to a mean potential. The molecules are treated as rodlike rigid bodies. In the uniaxial mesophases (N or Sm-A) this theory predicts for the planar alignment two modes that can be detected dielectrically. One is related to the rotation around the molecular long axis and then to the transverse dipole moment, and the other to the precession of the long axis around the director of the phase and then to the longitudinal dipole moment. However, the frequencies of both modes are similar and the aspect of the relaxation is just a broad peak. Librations as well as conformational changes could also contribute to this relaxation. For the homeotropic alignment the main contribution is related to the reorientation of the long molecular axis around short axis and then with the longitudinal dipole moment. The frequency of this mode is lower than the one in the planar alignment and shows in general a high activation energy due to the nematic or smectic potentials. If the alignment is not good or the phase is tilted (for example, a Sm-C phase with the layer normal parallel to the electrodes) a superposition of all modes will be observed in the planar alignment (see, for example, Ref. [26]).

Figures 6(a)–6(c) are typical spectra in the AF, Sm-C^*_γ and Sm-C^*_A mesophases. In the I phase we observed two relaxations. The high frequency one is mainly related to the rotation around the molecular long axis and the low frequency one to the reorientation of the long molecular axis around short axis. These frequencies are different due to the anisotropy of the rotational diffusion tensor. On the other hand, the strength of the high frequency contribution is larger than that of the low frequency one, as was expected from the structure of the molecules of the compound. The parameters of the two modes in this phase have been deduced from the fitting of the complex dielectric permittivity to

$$\varepsilon(\omega)=\Delta\varepsilon_l(\omega)+\Delta\varepsilon_t(\omega)+\varepsilon_\infty-i\sigma_{\mathrm{dc}}/\omega, \qquad (3)$$

where $\Delta\varepsilon_l(\omega)$ stands for the contribution due to the mechanism relaxing in the low frequency side (l means longitudinal dipole moment), $\Delta\varepsilon_t(\omega)$ for the high frequency one (t means transverse dipole moment), ε_∞ for the residual high frequency permittivity after the relaxation of both, and σ_{dc}

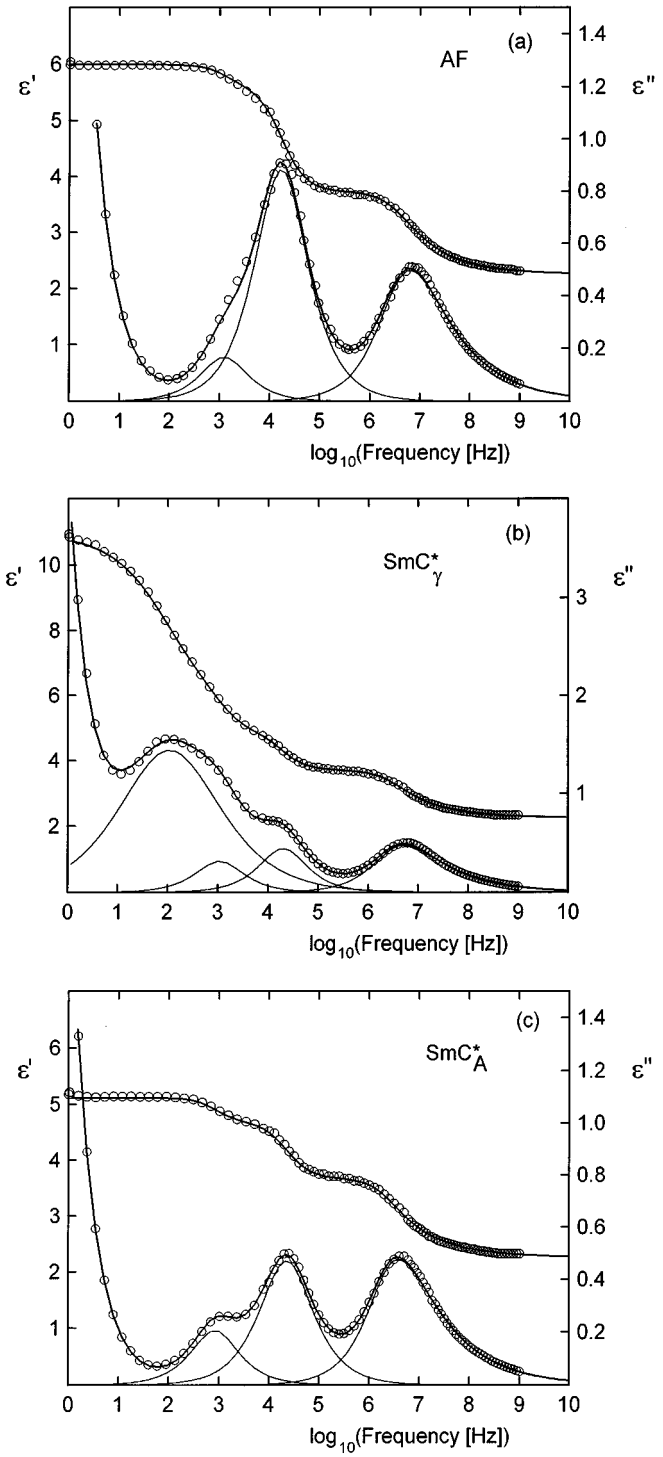

FIG. 6. (○) complex dielectric permittivity. Solid lines: fittings of the different modes. (a) AF phase, (b) Sm-C^*_γ phase, (c) Sm-C^*_A phase.

for the dc conductivity. Both relaxations were fitted to the Havriliak-Negami equation ($j=t,l$)

$$\Delta\varepsilon_j(\omega)=\Delta\varepsilon_j\,\frac{1}{[1+(i\omega\tau)^{\alpha}]^{\beta}}\,. \tag{4}$$

The α,β parameters of $\Delta\varepsilon_l(\omega)$ are unity (Debye behavior). The high frequency relaxation is broader an asymmetric ($\alpha\simeq 0.94$, $\beta\simeq 0.6$).

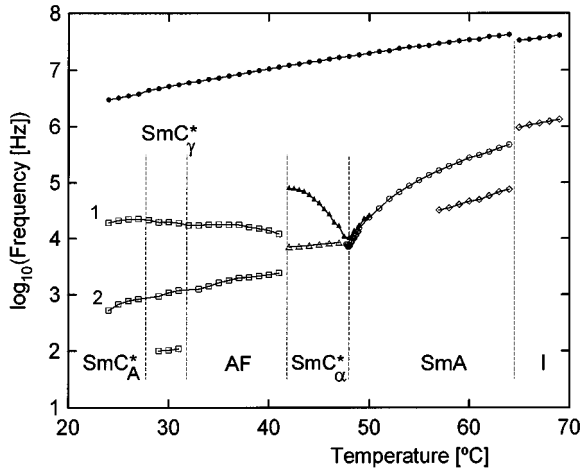

FIG. 7. Frequency of the different modes (deduced from the fittings) vs temperature. (●) rotation around the molecular long axis, (◇) rotation around the molecular short axis, (○) soft mode, (▲) soft mode with $E_{\rm dc}=1.4$ V μm^{-1}, (△) Goldstone mode, (□) modes 1, 2 and the ferrielectric Goldstone mode (see text).

In the Sm-*A* phase, apart from the relaxation related to the overall rotation around molecular long axis, which is observed in all phases, we observed two different relaxations. Near the *I* phase both have a small strength, but on decreasing the temperature the strength of the high frequency one increases while the other remains constant. The high frequency one is the soft mode (collective tilt fluctuations; that is, fluctuations of the director around layer normal) as can be deduced from the temperature behavior of its strength and frequency. The other relaxation is attributed to the reorientation of the molecular long axis around the short axis. We could only study it near the *I* phase because for lower temperatures it is hidden by the soft mode, not only because of the relative strengths but also due to the confluence of the frequencies (see Fig. 7). In this mesophase experimental data were also fitted to Eq. (3) but adding one more contribution to account for the soft mode $\Delta\varepsilon_s(\omega)$. This has a Cole-Cole behavior ($\beta=1$, the shape of the dielectric losses is symmetric) but near Debye type ($\alpha\simeq 1$).

In the Sm-C^*_α phase the main contribution in the low frequency side is related to a relaxation whose frequency is almost constant during the 6° of mesophase (10^4 Hz). As we shall show later this relaxation is a Goldstone mode. If there is also a soft mode, it is hidden by the Goldstone mode. The critical field needed to quench the Goldstone mode is quite high (1.2 V μm^{-1}), which is in accordance with the existence of a very short pitch. Due to the physical limit of 35 $V_{\rm dc}$ of our experimental device we checked this with thinner samples (25 μm). In this case another mode is observable during several degrees. Its behavior, both the strength and the frequency, joints with the soft mode of the Sm-*A* phase showing the typical ''*V*'' shape. Thus, in this phase the results were fitted to

$$\varepsilon(\omega)=\Delta\varepsilon_G(\omega)+\Delta\varepsilon_t(\omega)+\varepsilon_\infty-i\sigma_{\rm dc}/\omega, \tag{5}$$

where $\Delta\varepsilon_G(\omega)$ stands for the Goldstone mode contribution. Its spectral shape is near Debye type.

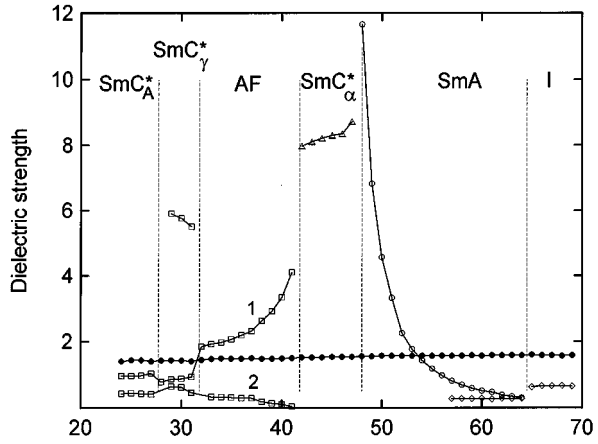

FIG. 8. Dielectric strength of the different modes (deduced from the fittings) vs temperature. Symbols are the same as in Fig. 8.

Figure 6(a) shows the real and imaginary components of the dielectric permittivity versus the logarithm of the frequency for a temperature in the AF phase. The spectrum is a little more complicated. The results were fitted to a superposition of three contributions: rotation around the molecular long axis $\Delta\varepsilon_t(\omega)$, and two modes that we will call $\Delta\varepsilon_{\mathrm{AF1}}(\omega)$ and $\Delta\varepsilon_{\mathrm{AF2}}(\omega)$. The last two are near Debye type.

In the Sm-C^*_γ phase [see Fig. 6(b)] we observed four relaxations. With respect to the preceding phase, one more relaxation has to be added in the very low frequency side (around 10^2 Hz). This relaxation is typical of these ferrielectric mesophases [10,12,15] and is called ''ferrielectric Goldstone mode'' because it is related to azimuthal reorientations of the director and can be easily quenched by means of a dc electric field. The shape of this relaxation, which we will call $\Delta\varepsilon_{\gamma G}(\omega)$, is Havriliak-Negami with $\alpha\simeq 0.6$ and $\beta\simeq 0.97$. Then the results were fitted to

$$\varepsilon(\omega)=\Delta\varepsilon_{\gamma G}(\omega)+\Delta\varepsilon_{\gamma 1}(\omega)+\Delta\varepsilon_{\gamma 2}(\omega)+\Delta\varepsilon_t(\omega)+\varepsilon_\infty - i\sigma_{\mathrm{dc}}/\omega. \tag{6}$$

In the Sm-C^*_A mesophase we observed three relaxations: $\Delta\varepsilon_t(\omega)$, $\Delta\varepsilon_{A1}(\omega)$, and $\Delta\varepsilon_{A2}(\omega)$ [see Fig. 6(c)]. These last two and the corresponding ones with similar frequencies in the Sm-C^*_γ and AF phases are near Debye type.

Figures 7 and 8 show the temperature dependence of the frequencies, and strengths of all the above mentioned modes. They have been deduced from the fittings and correspond to the experimental data with the 50 μm thick cells. We also include the frequencies of the mode assigned to the soft mode after quenching the Goldstone mode in the Sm-C^*_α phase, obtained with the 25 μm cells. At this point it is worth noticing that there could be some doubt about the strength and frequency of the mode $\gamma 2$ due to the large strength of the mode γG.

DISCUSSION

ICOOET is, to the best of our knowledge, the first compound with the naphthalene group instead of the biphenyl one showing antiferro and ferrielectric mesophases [27]. Some empirical rules related to the chemical structure and antiferroelectric ordering have been proposed [19]. This compound and the biphenyl analogous (MHDOBBC) [3,14] fulfill these rules. Both systems favor zigzag conformations of the molecules that induce tilted mesophases. Their length and polarizability exert a positive influence over the intermolecular interactions favoring the mesophase formation. However, their phase sequence and transition temperatures are different. In comparison with the linear geometry of the 4-4′ biphenyl system, the 2,6-disubstituted naphthalene ring allows us to introduce a step that significantly alters the linearity of the molecule. The naphthalene system is broader and increases the excluded volume of the whole molecule, giving rise to a decrease of the intermolecular forces. This effect lowers the mesophase temperatures, so for this compound it is possible to find a Sm-C^*_A phase at almost room temperature. In addition it has a broad range of Sm-C^*_α phase and re-entrant antiferroelectric mesophase (AF).

As mentioned by other authors, no texture changes at the Sm-$A\rightarrow$Sm-C^*_α phase transition could be seen [28,29]. We could not observe any dechiralization line indicating that or the Sm-C^*_α phase is not helicoidal or the pitch is very short. The pseudohomeotropic texture looks very uniform, which is also consistent with a very short pitch. This fact is in accordance with the results of other authors indicating that this phase is tilted, being the tilt of the molecules helicoidally modulated over only a few layers [15,23]. Then, the observed relaxation should be a superposition of the Goldstone mode and the soft mode. The strength of the Goldstone mode is much smaller than in Sm-C^* phases. For example, in this case it is around 8, and in the Sm-C^* phase of the homologous biphenyl compound it is around 150 [14]. On the other side, the critical field to quench the Goldstone mode is high, around 1.2 V $\mu\mathrm{m}^{-1}$: the pitch is short, then it is difficult to unwind the helix. In this case unwinding the helix should mean that the field induces at least partially the ferroelectric state. This is in accordance with the tilt measurements [Fig. 4(a)]: for 47 °C the steepest increase corresponds to a field that is around this value. We take the Sm-$A\rightarrow$Sm-C^*_α transition temperature T_c at the maximum value of the low frequency permittivity. It corresponds with the minimum value of the frequency (Fig. 7). After this point, the strength of the relaxation (Fig. 8) decreases while the frequency increases during 0.3°, and after, both frequency and strength rest almost constant. All these facts could be explained in the context of the standard mean field theory for the Sm-$A\rightarrow$Sm-C^* phase transition, which predicts the following behavior for the strength [Eq. 7(a)] and frequency [Eq. 7(b)] of the soft mode in the Sm-A [30]:

$$\Delta\varepsilon_{sA}\approx\frac{1}{\alpha(T-T_c)+Aq_0^2}, \tag{7a}$$

$$f_{sA}\approx\alpha(T-T_c)+Aq_0^2, \tag{7b}$$

where A and α are constants of the model and q_0 is the wave vector of the pitch at T_c. In the Sm-C^* phase the soft mode parameters are given by Eqs. 7(a) and 7(b), replacing $\alpha(T-T_c)$ by $2\alpha(T-T_c)$. The strength [Eq. 8(a)] and frequency [Eq. 8(b)] of the Goldstone mode are given by

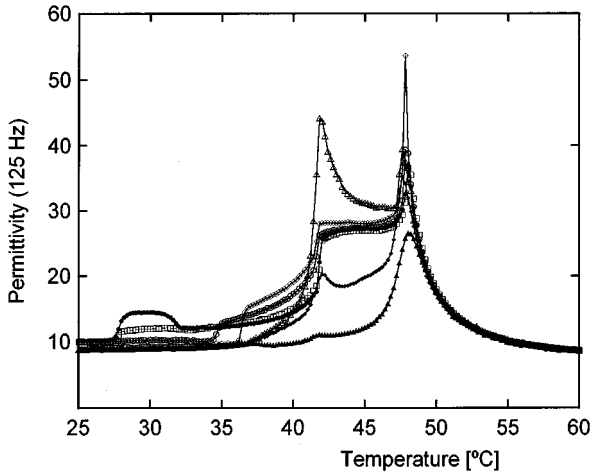

FIG. 9. Dielectric permittivity at 125 Hz (on cooling) vs temperature for different bias fields: (●) 0 V μm^{-1}, (□) 0.2 V μm^{-1}, (○) 0.4 V μm^{-1}, (◇) 0.6 V μm^{-1}, (△) 0.92 V μm^{-1}, (◆) 1 V μm^{-1}, (▲) 1.4 V μm^{-1}.

$$\Delta\varepsilon_G \approx \frac{1}{q^2}, \tag{8a}$$

$$f_G \approx q^2. \tag{8b}$$

If the Sm-C^*_α phase is interpreted as a Sm-C^* with a very short pitch, the high value of the Goldstone mode frequency and also the small value of its strength are clear. Just around the Sm-$C^*_\alpha \rightarrow$Sm-A phase transition the situation is not clear. Probably in the first 0.3 °C after the phase transition the relaxation is a mixture of soft mode and Goldstone mode. Note that the soft mode strength around the transition is quite large even with a dc field (Fig. 9) and also that the Goldstone mode frequency is higher than the soft mode frequency at the transition.

In Fig. 9 we have represented ε' at 125 Hz versus temperature for several bias fields from 0 to 1.4 V μm^{-1} (with a cell thickness of 25 μm). It is clear, when one compares the results of 0.92 V μm^{-1} with the results when $E_{dc}<0.92$ V μm^{-1}, that something strange has happened. The maximum permittivity value at the Sm-$A \rightarrow$Sm-C^*_α phase transition increases with increasing field till $E_{dc}=0.92$ V μm^{-1} and after decreases. This decrease indicates that the field is unwinding the helix and quenching the Goldstone mode. This fact was corroborated by the optical observation. For E_{dc} between 0.8 and 0.92 V μm^{-1} clear dechiralization lines appear under the polarizing microscope: the field is making the pitch longer and then the Goldstone mode strength would become larger. For higher fields the helix becomes unwound and the Goldstone mode disappears. The measurements with 1.4 V μm^{-1} shows a behavior typical of a soft mode contribution. For these cells and with $E_{dc}=1.4$ V μm^{-1} we obtained the temperature dependence of the soft mode around the Sm-$A \rightarrow$Sm-C^*_α phase transition that we have represented in Fig. 7 (closed triangle). For $E_{dc}=0.92$ V μm^{-1} the permittivity exhibits a sharp maximum for a temperature near the zero field Sm-$C^*_\alpha \rightarrow$AF phase transition. This maximum is due to the Goldstone mode. Its frequency is the same as at zero field.

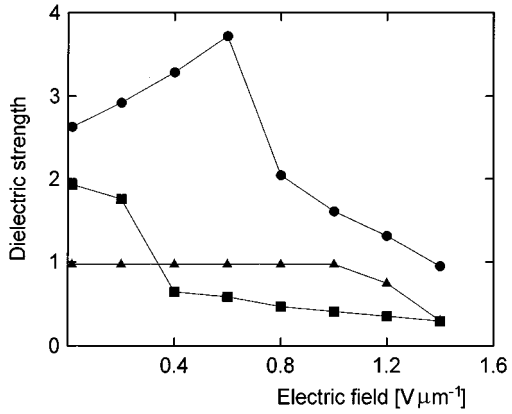

FIG. 10. Dielectric strength of mode 1 versus bias field in both antiferroelectric mesophases: (●) 38 °C (AF), (■) 33 °C (AF), (▲) 26 °C (Sm-C^*_A).

In the AF phase the permittivity shows a decrease. In the low frequency range we obtained two relaxations [see Fig. 6(a)]. The one with the lower frequency and smaller strength (AF2) shows thermal activation and has a continuity in the following Sm-$C^*_\gamma(\gamma 2)$ and Sm-$C^*_A(A2)$ phases. We think that it could be due to the rotation around the molecular short axis. Note that in tilted and helical structures this mechanism contributes to the planar permittivity, and also it could be present due to misalignments. Note that the frequency (10^3–10^4 Hz) is lower than in other compounds with smectic mesophases [31–35]. The dielectric strength of the relaxation that takes place at 10^4 Hz and identified as AF1 decreases on decreasing temperature and its frequency increases with a jump at the Sm-$C^*_\alpha \rightarrow$AF phase transition. In the Sm-C^*_γ and Sm-C^*_A phases we also observe a mode with similar frequency ($\gamma 1$ and $A1$) but there is a jump in frequency and strength at the AF$\rightarrow$Sm-C^*_γ phase transition. The jump of the strength is very clear but the jump of the frequency could be an artifact of the fitting procedure [see Fig. 6(b), the low frequency mode is very large]. In order to analyze its nature we studied its behavior under different bias fields for different temperatures in different phases (see Fig. 10, cell thickness of 25 μm). The frequency is not noticeably changed by the dc fields but the strength is. This phase is helical; the dechiralization lines are very clear under the polarizing microscope. However, its behavior under bias fields is very complex above all near the Sm-C^*_α phase. The helix is easily unwound (0.4 V μm^{-1}) but a larger field 0.7 V μm^{-1} produces another helix. A further increase of the field unwinds this helix. Coming back to the AF1 mode, at 38 °C in the AF phase for low fields the strength shows a linear increase and for E_{dc} between 0.6 and 0.8 V μm^{-1} an important decrease with a jump, in the same way as other authors obtained for the Sm-C^*_A phase [16]. This jump depends on the temperature and takes place at the field where the ''field-induced'' dechiralization lines disappear. The lower the temperature the smaller the jump and the field at which takes place. It is worth noticing that in the low temperature side of the AF phase after unwinding the helix it does not appear after switching off the bias field. In this temperature region the strength of the AF1 mode does not show an increase for low fields (see Figs. 9 and 10 for

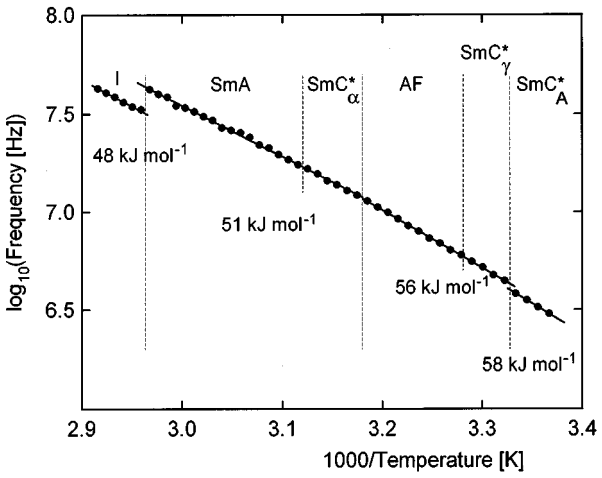

FIG. 11. Arrhenius plot of the frequency of the mode related to the rotation around the molecular long axis.

33 °C). We think that this mode could be understood as an azimuthal in antiphase reorientation of the director with constant tilt [8], being directly related to the antiferroelectric ordering. This would also explain the decrease at the AF→Sm-C^*_γ phase transition (see Fig. 8). For all temperatures in the AF phase a low frequency relaxation appears when the strength of the AF1 mode shows the jump. The latter relaxation could be the ferrielectric Goldstone mode. In the Sm-C^*_A phase it is almost constant till $E_{dc}=1$ V μm^{-1}, where it shows a decrease. This field corresponds to the critical field needed to suppress the helix as it was corroborated by the optical observation. It also corresponds to the increase of the apparent tilt angle [Fig. 4(a)]. Then it seems that this mode is related to both the antiferroelectric ordering and the helical structure.

With respect to the high frequency relaxation, which was assigned to the overall molecular reorientations around long axis, some comments are needed. In other ferroelectric liquid crystals with the usual Sm-*A*→Sm-*C** phase transition this mode shows a broader spectral shape and in general its frequency does not show any jump at the phase transitions, neither at the isotropic→smectic (or cholesteric) nor among different smectic mesophases [31–35]. This mode, in general, shows thermal activation with activation energies around 30 kJ mol^{-1}. Figure 11 is an Arrhenius plot [$\log_{10}(f_t)$ vs 1000/T] of the frequency of this mode. The frequency is lower than in other materials and the activation energy larger. There is a jump (an increase) at the *I*→Sm-*A* phase transition, according to the theoretical predictions. To the best of our knowledge this fact was never observed for smectics. We think that could imply that the molecular structure of ICOOET, and probably other materials showing antiferroelectric phases, is more rigid than in other ferroelectrics and then they are nearer the theoretical assumptions of the rotational diffusion model. The order parameter of the long molecular axis should be large (note the important jump at the *I*→Sm-*A* phase transition of the frequency of the mode related to the reorientations around short molecular axes, Fig. 7). Another important point is that the spectral shape is in accordance with the Havriliak-Negami equation in the whole temperature range from the *I* to the Sm-C^*_A phase. This spectral shape does not change at the transitions. The values of the α, β parameters in Eq. (4) are around 0.94 and 0.6 everywhere. Note that this relaxation has been well characterized because, even the *I* phase is well inside the experimental frequency window. It seems that this *a priori* empirical relaxation shape is a characteristic of this mechanism and not a consequence of a superposition of different relaxations (conformational changes, librations, etc.) with similar frequencies. The activation energy in the Sm-*A* and Sm-C^*_α phases is the same (51 kJ mol^{-1}) and also in the AF and Sm-C^*_γ phases (56 kJ mol^{-1}) with no jumps of the frequency at the transitions. However, at the Sm-C^*_γ→Sm-C^*_A phase transition there is a jump, but the activation energy is almost the same. This could indicate that the pairing of transverse dipole moments, proposed to account for the structure of this mesophase, has some importance in the dynamics of the rotation around long molecular axis. In this sense, recently it has been proposed for MHPOBC [36] that in the Sm-C^*_A phase of this material the carbonyl group near the chiral center lies on the tilt plane while in the Sm-*C** phase it takes a considerably upright position. Probably this different main position could influence the hindered motion of molecules around molecular long axis. The dielectric results could suggest that there is more order of the molecular transverse axes.

In summary, we have analyzed by means of optical, dielectric, and calorimetric studies a compound exhibiting several subphases derived from the Sm-*C** phase. In particular it has a relatively broad range of Sm-C^*_α phase and a reentrant antiferroelectric one. This compound shows a rich and complex dielectric response with several active modes in each subphase. We have analyzed the temperature and field behavior of some of these modes. However, much effort has to be done, not only in this material, to clarify the origin of some of these modes. The field-induced phase transition makes this type of study a difficult task.

ACKNOWLEDGMENTS

This work was supported by the Spanish Government (Projects Nos. CICYT MAT-94-0717-C02-02 and DGCYT PB91-0554). S. Merino thanks the Basque Government.

[1] A. D. L. Chandani, Y. Ouchi, H. Takezoe, A. Fukuda, K. Terashima, K. Furukawa, and A. Kishi, Jpn. J. Appl. Phys. **28**, L1265 (1989).

[2] A. D. L. Chandani, E. Gorecka, Y. Ouchi, Takezoe, and A. Fukuda, Jpn. J. Appl. Phys. **28**, L1265 (1989).

[3] J. W. Goodby, J. S. Patel, and E. Chin, J. Mater. Chem. **2**, 197 (1992).

[4] V. L. Lorman, A. A. Bulbitch, and P. Toledano, Phys. Rev. E **49**, 1367 (1994).

[5] J. Li, H. Takezoe, and A. Fukuda, Jpn. J. Appl. Phys. **30**, 532

(1991).
[6] K. Hiraoka, A. Taguchi, Y. Ouchi, H. Takezoe, and A. Fukuda, Jpn. J. Appl. Phys. **29**, L103 (1990).
[7] S. Hiller, S. A. Pikin, W. Haase, J. W. Goodby, and I. Nishiyama, Jpn. J. Appl. Phys. **33**, L1170 (1994).
[8] K. Hiraoka, H. Takezoe, and A. Fukuda, Ferroelectrics **147**, 13 (1993).
[9] P. Gisse, J. Pavel, H. T. Nguyen, and V. L. Lorman, Ferroelectrics **147**, 27 (1993).
[10] M. Cepic, G. Heppke, J. M. Hollidt, D. Lötzsch, and B. Zeks, Ferroelectrics **147**, 159 (1993).
[11] M. Glogarová, H. Sverenyák, H. T. Nguyen, and C. Destrade, Ferroelectrics **147**, 43 (1993).
[12] S. Hiller, S. A. Pikin, W. Haase, J. W. Goodby, and I. Nishiyama, Jpn. J. Appl. Phys. **33**, L1096 (1994).
[13] H. Moritake, Y. Uchiyama, K. Myojin, M. Ozaki, and K. Yoshino, Ferroelectrics **147**, 53 (1993).
[14] M. R. de la Fuente, S. Merino, Y. González, B. Ros, J. A. Puértolas, and M. Castro, Adv. Mater. **7**, 564 (1995).
[15] M. Cepic, G. Heppke, J. M. Hollidt, D. Lötzsch, D. Moro, and B. Zeks, Mol. Cryst. Liq. Cryst. **263**, 207 (1995).
[16] M. Buivydas, F. Gouda, S. T. Lagerwall, and B. Stebler, Liq. Cryst. **18**, 879 (1995).
[17] A. Mochizuki, K. Motoyoshi, and N. Masakatsu, Ferroelectrics **122**, 37 (1991).
[18] N. Okabe, Y. Suzuki, I. Kawamura, T. Isozaki, H. Takezoe, and A. Fukuda, Jpn. J. Appl. Phys. **31**, L793 (1992).
[19] A. Fukuda, Y. Takanishi, K. Ishikawa, and H. Takezoe, J. Mater. Chem. **4**, 997 (1994).
[20] M. Cepic and B. Zeks, Mol. Cryst. Liq. Cryst. **263**, 61 (1995).
[21] H. Sun, H. Orihara, and Y. Ishibashi, J. Phys. Soc. Jpn. **62**, 2706 (1993).
[22] T. Isozaki, K. Hiraoka, Y. Takanishi, H. Takezoe, A. Fukuda, Y. Suzuki, I. Kawamura, Liq. Cryst. **12**, 59 (1992); T. Isozaki, T. Fujikawa, H. Takezoe, A. Fukuda, T. Hagiwara, Y. Suzuki, and I. Kawamura, Phys. Rev. B **48**, 13439 (1993).
[23] O. Mitsunobu, Synthesis **1**, 1 (1981).
[24] K. Hiraoka, Y. Takanishi, K. Skarp, H. Takezoe, and A. Fukuda, Jpn. J. Appl. Phys. **30**, L1819 (1991).
[25] Y. P. Panarin, H. Xu, S. T. MacLughadha, J. K. Vij, A. J. Seed, M. Hird, and J. W. Goodby, J. Phys. Condens. Matter **7**, L351 (1995).
[26] See, for example, G. Williams, in *The Molecular Dynamics of Liquid Crystals*, Vol. 431 of *NATO Advanced Study Institute*, edited by G. Luckhurst and C. A. Veracini (Kluwer, Dordrecht, 1994), Chap. 17.
[27] In the book of abstracts of the 15th International Liquid Crystal Conference (Budapest), J-Sbp25 (1994), a series of naphthalene derivatives is reported. Some of the members show the Sm-C_A^* phase instead of the Sm-C^* one.
[28] J. Philip, J. R. Lalanne, J. P. Marcerou, and G. Sigaud, J. Phys. II **4**, 2149 (1994).
[29] J. Philip, J. R. Lalanne, J. P. Marcerou, and G. Sigaud, Phys. Rev. E. **52**, 1846 (1995).
[30] T. Carlsson, B. Zeks, C. Filipic, and A. Levstik, Phys. Rev. A **42**, 877 (1990).
[31] M. R. de la Fuente, M. A. Pérez Jubindo, J. Zubia, T. Pérez Iglesias, and A. Seoane, Liq. Cryst. **16**, 1051 (1994).
[32] M. A. Pérez Jubindo, M. R. de la Fuente, and M. Marcos, Adv. Mater. **6**, 941 (1994).
[33] M. R. de la Fuente, S. Merino, M. A. Pérez Jubindo, and M. T. Sierra, Mol. Cryst. Liq. Cryst. **259**, 1 (1995).
[34] Y. González, B. Palacios, M. A. Pérez Jubindo, M. R. de la Fuente, and J. L. Serrano, Phys. Rev. E **52**, R5764 (1995).
[35] A. Schönfeld, F. Kremer, and R. Zentel, Liq. Crist. **13**, 403 (1993).
[36] K. Miyachi, J. Matsushima, Y. Takanishi, K. Ishikawa, H. Takezoe, and A. Fukuda, Phys. Rev. E **52**, R2153 (1995).